

SEGMENTATION OF THE SOLID BED IN INFRARED IMAGE SEQUENCES OF ROTARY KILNS

Patrick Waibel, Jörg Matthes and Hubert B. Keller
*Institute for Applied Computer Science, Karlsruhe Institute of Technology
Hermann-von-Helmholtz-Platz 1, 76344 Eggenstein-Leopoldshafen, Germany*

Keywords: Rotary kiln, Solid bed, Segmentation, Infrared camera.

Abstract: This paper presents two novel methods for segmenting the solid bed in infrared image sequences of metal-recycling rotary kilns. Exploiting the different dynamics and temperatures of gas phase, solid bed and kiln wall, we developed filter chains for an image segmentation of the solid bed. For the image acquisition we employed infrared cameras with a spectral filter. Two image processing algorithms were realized according to the two most common camera positions (frontal and top-left view on the solid bed at the rear-end of the kiln). Results show that both algorithms are capable to segment the solid bed in the image sequences accurately and reliably. The work presented here provides a basis for the extraction of characteristic process state variables, that can help to improve the process control with regard to product quality, energy consumption and emission reduction.

1 INTRODUCTION

Rotary kilns are industrially used for processing materials at high temperatures. Reducing the energy consumption, improving the product quality and lowering pollutant emission are important goals for the operation of rotary kiln plants. A new approach to achieve these goals is an advanced process control that uses additional information from cameras that capture images from the inside of the kiln. An appropriate image processing system is necessary to extract meaningful information of the process state out of the camera images to be used for the process control.

A rotary kiln is a cylindrical vessel that is slightly inclined to the horizontal. While the raw material is mixed by the rotating movement the solids gradually move towards the kiln's lower end. High temperatures are attained by a burner inside the kiln and exothermic reactions of the material. Infrared cameras are capable to capture the spatial arrangement of the solid bed and the temperature distribution inside the kiln all at once. An image processing system can enhance the benefit of the acquired images by identifying specific process parameters, e.g. filling height, repose angle or movement pattern of the solids (Henein et al., 1983). Due to varying process conditions the robustness of the applied image processing algorithms is an important factor. In this paper we address the prob-

lem of segmenting the solid bed in infrared-images of metal-recycling rotary kilns from the two most common camera positions (frontal and displaced to the top-left).

(Zipser et al., 2006) describe a software tool for monitoring and analyzing of video and infrared images of combustion processes. In (He et al., 2009) an intensity-based Fuzzy-C-Means clustering algorithm for segmenting the solid bed in video images of alumina kilns is presented. (Sun et al., 2008) examine the segmentation of the solid bed and burner flame in video images based on texture information and Fuzzy-C-Means clustering. Our segmentation algorithms process infrared images and make use of intensity as well as dynamic properties in a particular filter chain to improve the overall segmentation results. After outlining the image acquisition in section 2 the image segmentation method developed for a frontal view position of the camera is described in section 3. Section 4 depicts the segmentation algorithm for a top-left view of the camera and section 5 concludes this paper.

2 IMAGE ACQUISITION

The analyzed image sequences were captured at a metal-recycling rotary kiln located in Freiberg (Ger-

many). The length of the kiln is 43m with an inner diameter of 3.6m. We used two different infrared-cameras, which were installed at the lower end of the kiln. The first camera (*scenario 1*) with a resolution of 256x128 pixels was located slightly below the rotational axis of the kiln (Figure 1 left). The second camera was installed at the top-left of the rotary axis (*scenario 2*). It has a resolution of 320x240 pixels (Figure 1 right). Both cameras are equipped with a spectral filter at 3.9 μ m where the absorbance of the burning gas atmosphere is at a minimum. The intensity values of the pixels correspond to absolute temperatures (400 to 2000°C) with an accuracy of ± 5 K. A developed image preprocessing system guarantees the validity of the acquired images. In the acquired image sequences the direction of rotation is anti-clockwise. Therefore the solid bed is moved upwards the right side of the kiln with regard to its current repose angle. On legal grounds, parts of the air supply unit had to be blacked out in the presented images.

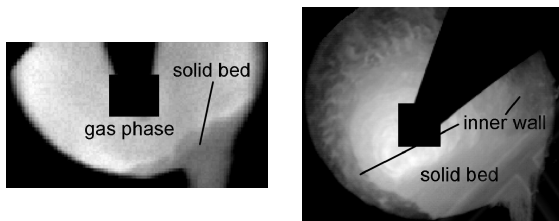


Figure 1: Scenario 1 (left) and Scenario 2 (right).

3 IMAGE SEGMENTATION - SCENARIO 1

3.1 Method

At lower average kiln temperatures the solid bed can easily be segmented via intensity differences, as the solid bed is colder than the gas phase in such situations. However, with increasing temperature the intensity differences of gas phase and solid bed vanish and a solely intensity-based segmentation algorithm fails (Figure 2). A robust filter algorithm has to handle both situation in an adequate way. The algorithm we developed makes use of different intensity properties as well as dynamic properties of the solid bed and the gas phase (Figure 3).

In the *intensity-based part* of the algorithm at first an *automatic thresholding* is performed on a region of interest (ROI) containing the possible locations of the solid bed. This method aims to find regions with homogeneous intensity values via multiple thresholding. Then all minimums in the intensity histogram of

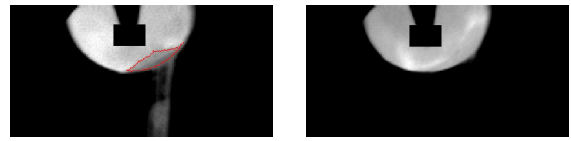


Figure 2: Simple threshold segmentation at low (left) and high (right) mean temperatures.

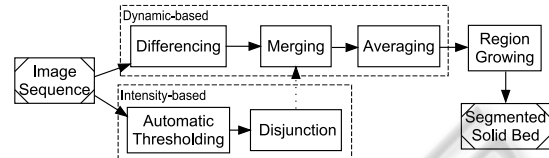


Figure 3: Solid bed segmentation algorithm for a frontal camera view on the kiln.

the ROI of a single image are located. Each minimum is used as a threshold segmentation. The segmented regions are subsequently examined if their mean intensity is below an offset (we used 30K) to the mean intensity of the entire ROI. Regions with mean intensities above this value are not further considered. The region with the highest permitted threshold is subdivided in connected pixel regions, whose areas (number of pixels) are computed. Connected regions with small areas (we used 30 pixels as threshold) are removed as fluctuations in the gas phase can generate these regions. Consequently, the remaining connected regions are defined as solid bed due to their mean intensities and sizes. A grouping of these regions ideally corresponds to the entire solid bed region. However, in many cases only a part of the solid bed is detected or there is no valid segmentation result at all (e.g. if the minimum search in the histogram is not successful). Therefore the dynamic properties of the solid bed and the gas phase are accounted for in the segmentation algorithm. The *dynamic-based part* is adapted from a modified calculation of the total variation (TV) of each pixel. Two temporally successive images are used to compute a difference image (*differencing*). The accumulated absolute differences of an image sequence reflects the total variation for each pixel which is an indicator for the fluctuation behavior of the intensity values. In our algorithm we normalize the total variation with the number of used frames in order to simplify the comparison of different frame limits. Therefore this step can be regarded as an *averaging* of the differences. The intensity values of the gas phase are usually more fluctuating than the solid bed's which leads to higher TVs in the gas phase region. Nevertheless it is possible that moving lumps within the solid bed, which are colder than the surrounding material, facilitate high TV values at their contours even inside the solid bed region. To circumvent this problem and to improve the overall seg-

mentation result the intensity-based part is addressed again. The *merging* step is the key element of the algorithm. The preliminary segmentation result of the intensity-based part is combined with the dynamic-based computations. Cold lumps within the solid bed are always either segmented solely or together with the rest of the bed by the automatic threshold step due to their low temperatures. The automatic thresholding is done with both images which are used for the respective differencing step. The pixels which are defined as solid bed in at least one of the images are approved as solid bed region in the *disjunction* step, i.e. a relocation of a lump can be captured. Now, all pixels included in the identified intensity-based solid bed region are set to 0 in the current difference image. This merging situationally leads to an enhanced distinguishability between the gas phase and solid bed in the averaged difference images. If the mean temperature of the kiln is high, the segmentation algorithm is predominantly based on the dynamics-based part since the intensity-based part rarely detects the solid bed region. When there is a high contrast between solid bed and gas phase in the input images the intensity-based part boosts the results of the dynamics-based part due to the merging step. Additionally, high difference values at the contours of moving lumps are prevented through this combination. For the final segmentation step a *region growing* algorithm is implemented.

3.2 Results and Discussion

In figure 2 segmentation results at the frontal view position with an fixed threshold segmentation are illustrated. The intensity-based threshold segmentation succeeds to detect the solid bed region in image sequences with low mean temperatures of the kiln. As soon as the temperature rises this method fails. Even an adaptive thresholding is not applicable at higher mean temperatures, as there are no intensity differences between gas phase and solid bed. Figure 4 shows segmentation results with the combined segmentation algorithm. They are each based on 200 frames. It can be seen that the modified averaged difference images possess high contrasts between solid bed and gas phase regions also at high mean temperatures of the kiln. This enables an accurate final segmentation with the region growing algorithm.

The developed combined segmentation filter chain proved to be a reliable and precise method to detect the solid bed in scenario 1 infrared images. This allows the extraction of process relevant solid bed features in future works. It is e.g. possible to define a circle segment with two parameters corresponding to

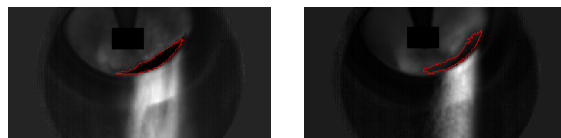


Figure 4: Segmentation with modified averaged difference images at low (left) and high (right) mean temperatures.

filling height and repose angle. In an iterative optimization process both parameters are adapted to find the best-fit of circle segment and segmented solid bed. Besides acquiring these two parameters, the remaining error between circle segment and solid bed region can be used to discriminate the bed movement (e.g. slumping or rolling).

4 Image Segmentation - Scenario 2

Conversely to scenario 1 in this case the solid bed has to be distinguished from the inner kiln wall instead of the gas phase. Intensity values cannot be used for the segmentation since the temperatures of kiln wall and solid bed are similar. Especially at the upper border of the solid bed, where solid parts stick to the wall, an intensity-based segmentation has little prospect of success. The filter chain we developed makes use of the different dynamic properties of the kiln wall and the solid bed. In particular we discriminate the steady rotating movement of the wall from the specific mixing movement of the solid bed.

4.1 Method

The first step of our segmentation process is a *mapping*. Two circles in the acquired images are set, in order to define the geometry of the inner surface of the kiln. Then a geometric mapping of the inner surface to a rectangle is performed (Figure 5 left). With the mapped intensity values a movement analysis is conducted. An optical-flow algorithm (Brox et al., 2004) computes a vector field out of two successive mapped images (Figure 5 right). Each vector specifies the direction and the magnitude of the movement of a pixel between two frames. Due to the mapping step the rotation of the kiln is transformed in a rightward movement. Consequently, discriminating the solid bed from the kiln wall corresponds to detecting the image region that is not constantly moving to the right. Since the material of the solid bed is also transported up along the kiln wall before it collapses respectively slides back in the opposite direction, an discrimination via movement is not possible at all times. Thus we implemented a moving average filter which averages the movements of the last

200 frames. In the so computed image the solid bed can be segmented with a simple threshold operator. Afterwards the segmented region in the mapped rectangular is mapped back to the original image. The single steps of the segmentation filter chain are illustrated in figure 6.

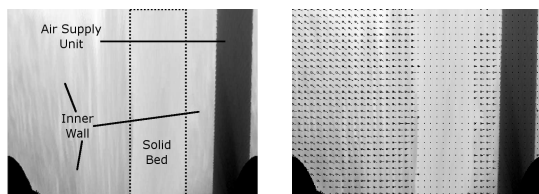


Figure 5: Mapping of kiln's inner surface to a rectangle (left) and vector field of mapped kiln's inner surface (right).

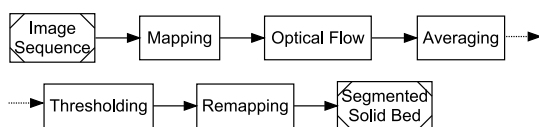


Figure 6: Solid bed segmentation algorithm for a camera view from top-left.

4.2 Results and Discussion

The averaged horizontal velocities of an image sequence are shown in figure 7 left. Brighter gray values correspond to higher velocities. Whereas the dark vertical stripe on the right side is due to the air supply unit, the dark stripe more to the left is caused by the dynamics of the solid bed. After a coarse definition of the ROI the lower part of the mapped solid bed is segmented via thresholding. The upper part is error-prone at some sequences because of the mapping process. Nevertheless the remapping of the segmented region in the original image achieves accurate results (Figure 7 right). In the next step extensions of the segmentation method will be examined. For instance, the best-fitting rectangular of the segmented region in the mapped horizontal velocities will be determined. This could improve the segmentation results in the more distant region of the solid bed. Additionally, the difference between the segmented region and the best-fitting rectangle could be used as an indicator for the particular movement pattern of the solid bed.

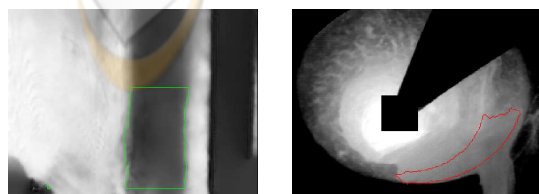


Figure 7: Averaged horizontal velocity values (left) and segmentation result (right).

5 CONCLUSIONS

The extraction of features from infrared image sequences of the inside of rotary kilns provides a high potential to improve the process control. An important requirement is the reliable and accurate segmentation of the specific regions in the acquired images. In this work we presented image segmentation filter chains that were capable to segment the solid bed in infrared images of a rotary kiln from the two most common camera positions. Results show that the combination of intensity-based and dynamic-based features considerably enhance the segmentation results at a frontal view position of the camera. From a top-left view on the solid bed the succession of a mapping process and an optical-flow computation enables satisfying segmentation results. In future works the correlation between extracted solid bed features with process states will be examined, particularly with regard to improvements for the process control.

REFERENCES

Brox, T., Bruhn, A., Papenberg, N., and Weickert, J. (2004). High accuracy optical flow estimation based on a theory for warping. In *ECCV*, pages 25–36.

He, M., Zhang, J., and Liu, X. (2009). Determination of the repose angle of stuff in rotary kiln based on imaging processing. In *ICEMI*, pages 4–97–4–101.

Henein, H., Brimacombe, J., and Watkinson, A. (1983). Experimental study of transverse bed motion in rotary kilns. *Metall. Trans. B*, 14(2):191–205.

Sun, P., Chaia, T., and jie Zhou, X. (2008). Rotary kiln flame image segmentation based on FCM and gabor wavelet based texture coarseness. In *WCICA*, pages 7615–7620.

Zipsper, S., Matthes, J., and Keller, H. (2006). Camera aided control of combustion processes with the software tool inspect. *at - Automatisierungstechnik*, 54:574–81.